

Second harmonic generation and enhancement in microfibers and loop resonators

Marcelo A. Gouveia, Timothy Lee, Rand Ismaeel, Ming Ding, Neil G. R. Broderick, Cristiano M. B. Cordeiro, and Gilberto Brambilla

Citation: [Applied Physics Letters](#) **102**, 201120 (2013); doi: 10.1063/1.4807767

View online: <http://dx.doi.org/10.1063/1.4807767>

View Table of Contents: <http://scitation.aip.org/content/aip/journal/apl/102/20?ver=pdfcov>

Published by the [AIP Publishing](#)

Articles you may be interested in

[Wide-range cyclic phase matching and second harmonic generation in whispering gallery resonators](#)

Appl. Phys. Lett. **103**, 181107 (2013); 10.1063/1.4827538

[Second harmonic generation in ridge Bragg reflection waveguides](#)

Appl. Phys. Lett. **92**, 101124 (2008); 10.1063/1.2894516

[Analysis of second harmonic generation in photonic-crystal-assisted waveguides](#)

J. Appl. Phys. **100**, 043110 (2006); 10.1063/1.2266104

[Enhancement of third-harmonic generation in a polymer-dispersed liquid-crystal grating](#)

Appl. Phys. Lett. **87**, 051102 (2005); 10.1063/1.1999849

[Optical second-harmonic generation in lead formate](#)

J. Appl. Phys. **87**, 22 (2000); 10.1063/1.371820



AIP | Journal of
Applied Physics

Journal of Applied Physics is pleased to
announce **André Anders** as its new Editor-in-Chief

Second harmonic generation and enhancement in microfibers and loop resonators

Marcelo A. Gouveia,^{1,2,a)} Timothy Lee,^{1,a)} Rand Ismaeel,^{1,a),b)} Ming Ding,¹ Neil G. R. Broderick,³ Cristiano M. B. Cordeiro,² and Gilberto Brambilla¹

¹Optoelectronics Research Centre, University of Southampton, Southampton SO17 1BJ, United Kingdom

²Instituto de Física “Gleb Wataghin,” Universidade Estadual de Campinas—UNICAMP, Campinas, São Paulo, Brazil

³Physics Department, University of Auckland, Private Bag 92019, Auckland 1142, New Zealand

(Received 18 March 2013; accepted 12 May 2013; published online 24 May 2013)

We model and experimentally investigate second harmonic generation in silica microfibers and loop resonators, in which the second order nonlinearity arises from the glass-air surface dipole and bulk multipole contributions. In the loop resonator, the recirculation of the pump light on resonance is used to increase the conversion. The effect of the loop parameters, such as coupling and loss, is theoretically studied to determine their influence on the resonance enhancement. Experimentally, microfibers were fabricated with diameters around $0.7\ \mu\text{m}$ to generate the intermodally phase matched second harmonic with an efficiency up to 4.2×10^{-8} when pumped with 5 ns $1.55\ \mu\text{m}$ pulses with a peak power of 90 W. After reconfiguring the microfiber into a 1 mm diameter loop, the efficiency was resonantly enhanced by 5.7 times. © 2013 AIP Publishing LLC. [<http://dx.doi.org/10.1063/1.4807767>]

Nonlinear effects of light in bulk media and waveguides have been a popular topic in the last few decades. Previous studies showed that focusing high power short pulses into crystals with higher order electric field polarizability could produce new frequencies related harmonically with the pump frequency and the material attributes. One application of these materials, such as Barium Borate, is in optical parametric oscillators and harmonic generation, where it is possible to manipulate the input signal (seed) in order to generate a wide range of wavelengths.¹

Optical fibers experience some restrictions imposed by the material: Silica is a centrosymmetric material and, therefore, has negligible bulk even-order polarization contributions. Yet, weak second harmonic generation (SHG) has been observed in optical fibres for pulsed sources with a peak power of the order of 70 kW.² Enhanced nonlinearity is usually achieved exploiting silica molecular arrangement, which can accommodate impurities—dopants. Moreover, with the development of photonic crystal fibers, the generation of specific wavelengths or broadband supercontinuum generation has been reported at high intensities.³

Recently, micro/nanofibers (MNFs) have been proposed for nonlinear applications because of the highly confined mode. MNFs are formed by simultaneously heating and pulling optical fibers, so the shape of the transition regions can be controlled to maintain an adiabatic diameter profile.⁴

For harmonic generation, MNFs can achieve the phase matching condition between different modes, by ensuring the correct diameter so the pump and harmonic modes share the same effective index. Third harmonic generation using MNFs has been reported with an efficiency up to 3×10^{-4} in

past literature.⁵ In the case of SHG, fortunately, it is possible to exploit the molecular anisotropy near the glass-air interface⁶ to provide a reasonable surface dipole contribution, as well as the bulk multipolar contributions.⁷

This present study demonstrates SHG in MNFs at sub-kW intensities and a simple technique to enhance its efficiency by configuring it into a loop resonator for pump recirculation. First, a theoretical approach for SHG in nonlinear MNF loop resonators and its theoretical efficiency enhancement will be introduced, followed by experimental data for a straight MNF and efficiency enhanced with a MNF loop resonator. This method is similar to that applied for THG (third harmonic generation) in MNF.⁸

To simulate the SHG in a silica microfiber, the model developed by Lægsgaard⁶ was used, in which the second order nonlinear polarization $\mathbf{P}^{(2)}$ includes not only the surface dipole contributions (which are dominant for narrower MNFs with a higher surface field intensity) but also the bulk multipolar components. The evolution of the pump and harmonic electric field amplitudes, $A_1(z)$ and $A_2(z)$, respectively, is governed by the following differential equations,⁶ adapted to incorporate self (SPM) and cross (XPM) phase modulation:

$$\frac{dA_1}{dz} = -\alpha A_1 + in_2 k_1 [(J_1 |A_1|^2 + 2J_2 |A_2|^2) A_1] + i\rho_2 A_2 A_1^* e^{-i\delta\beta z}, \quad (1)$$

$$\frac{dA_2}{dz} = -\alpha A_2 + in_2 k_1 [(4J_2 |A_1|^2 + 2J_5 |A_2|^2) A_2] + i\rho_2 A_1^2 e^{i\delta\beta z}, \quad (2)$$

where $k_1 = 2\pi/\lambda$ is the pump free space propagation constant; $\delta\beta = \beta_2 - 2\beta_1$ is the detuning (between the harmonic and the pump propagation constants β_2 and β_1 , respectively); n_2 is the silica nonlinear refractive index; α is the loss; J_1, J_2, J_5

^{a)}M. A. Gouveia, T. Lee, and R. Ismaeel contributed equally to this work.

^{b)}Author to whom correspondence should be addressed. Electronic mail: rmni1g10@orc.soton.ac.uk

denote the overlap integrals for the pump SPM, XPM, and harmonic SPM, respectively;⁸ and ρ_2 is the overlap integral between the harmonic mode field and $\mathbf{P}^{(2)}$. A MNF diameter of $0.78 \mu\text{m}$ is assumed, such that the $\text{HE}_{11}(\omega)$ pump mode at $\lambda_\omega = 1.55 \mu\text{m}$ is phase matched with the $\text{HE}_{21}(2\omega)$ harmonic mode, for which $\rho_2 = 0.11 \text{ m}^{-1} \text{ W}^{-1/2}$. Although the taper waist is generally several mm long, the region with the required phase matching diameter is in practice much shorter, as discussed later, and hence we choose a harmonic interaction length of $L_{\text{SH}} = 200 \mu\text{m}$, deduced from the profile of the experimentally fabricated tapers. A detuning of $\delta\beta = -100 \text{ m}^{-1}$ was chosen to be near the optimum value needed to compensate for phase modulation.

For an input power of $P_0 = 200 \text{ W}$, the predicted efficiency for the straight MNF case is $\eta = 7.6 \times 10^{-8}$. Although higher conversions are possible since η would increase linearly with either L_{SH} or P_0 , here we focus on low powers to minimise nonlinear pump broadening in experiments so that the resonant enhancement can be more clearly observed.

When the MNF is configured into a loop, the close proximity of the microfiber segments introduces a coupling region of length L_c with coupling coefficient κ_ω between the pump modes (the higher order harmonic mode transverse field profile contains more zeroes over and hence its coupling is weaker, so it is assumed off-resonance with $\kappa_{2\omega} = 0$). Equations (1) and (2) are thus modified to incorporate the linear coupling along L_c , and solved numerically with boundary conditions based on the continuity of the recirculated amplitudes.⁹ The resonance is strongest at critical coupling when the overall power coupling $K = \kappa_\omega L_c$ equals $\pi(m + 1/2)$ for integer m ,¹⁰ with the lowest value at $K_c = 3\pi/2$. In experiments, it is possible to achieve close proximity to critical coupling, i.e., small $\Delta K = K_c - K$, and Fig. 1 shows the linear spectrum and nonlinear pump/harmonic spectra when the pump is detuned from a resonance near $\sim 1.55 \mu\text{m}$ with $\Delta K = 0.81$ (chosen to match the linear transmission of the experimental loops). The total loop MNF

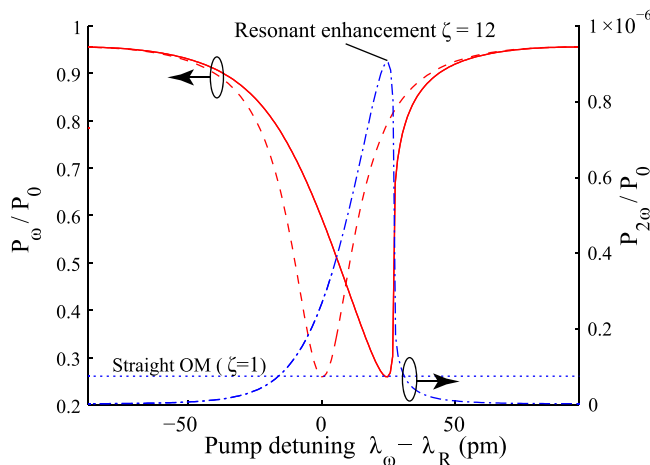


FIG. 1. Simulated loop output showing the linear pump (dashed), nonlinear pump (solid) and second harmonic (dotted-dashed) transmission, when the pump wavelength λ_ω is detuned from a resonance near $\lambda \approx 1.55 \mu\text{m}$. The dotted line shows the SHG conversion from a corresponding straight MNF. Parameters: loop length = 12 mm , $L_{\text{SH}} = 200 \mu\text{m}$, $P_0 = 200 \text{ W}$, $\Delta K = 0.81$ ($\kappa_\omega = 7.8 \times 10^4 \text{ m}^{-1}$, $L_c = 50 \mu\text{m}$), $\alpha = 10 \text{ m}^{-1}$.

length is 12 mm , within which SHG is assumed to occur over $200 \mu\text{m}$ as before.

The nonlinear resonance occurs at a longer detuning than the linear case due primarily to SPM, which would also be responsible for hysteresis at higher powers. Compared to the efficiency from the straight MNF, the conversion can be enhanced by up to $\zeta = 12$ times due to the higher pump field strength within the loop on resonance. Note that the enhancement bandwidth, approximately 20 pm at the full-width half-maximum (FWHM) level, is primarily governed by the resonance linewidth, and far from resonance ζ can fall below unity due to the pump bypassing the loop.

Higher ζ can be achieved in loops closer to K_c (smaller ΔK), as shown in Fig. 2(a). As an example, in the low loss case of $\alpha = 1 \text{ m}^{-1}$, the recirculating power P_{circ} can be over eight times greater than P_0 when $\Delta K = 0.7$, which consequently provides a large $\zeta = 64$ (18 dB) enhancement given in Fig. 2(b). Here, in the undepleted pump regime, the enhancement is roughly $\zeta \approx (P_{\text{circ}}/P_0)^2$. Although ζ falls with increasing loss, the enhancement remains significant even for higher losses of $\alpha = 10 \text{ m}^{-1}$, and for this reason any minor loss incurred during the manufacture of the loop, such as surface contamination/scattering, is likely to be offset by the subsequent resonant enhancement.

Before proceeding with the experimental details, it is necessary to introduce the fiber based source used for this study, since the SHG depends on the sample conditions, e.g., phase-matching conditions, and the pump power. The source diagram depicted in Fig. 3 consists of a tunable laser source (TLS) set at 1550 nm connected to three amplifiers, an electronic optical modulator (EOM) in order to produce 5 ns pulses, and an acoustic optical modulator (AOM) which removes the unwanted background amplified spontaneous emission generated by the Amonics amplifier. The last amplifier, an erbium doped fiber amplifier (EDFA), is used to increase the peak pulse power up to $P_0 = 1 \text{ kW}$.

First, a MNF satisfying the phase matching condition for SHG was fabricated by placing a single mode fiber (SMF 28) on a translation stage where the fiber undergoes heating as well as pulling, to produce a MNF with adiabatic transition regions. One of the fiber ends was connected to the pulsed source described above whilst the other end was

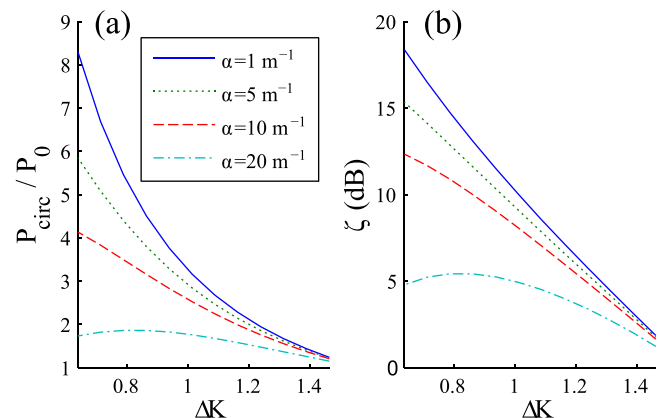


FIG. 2. (a) The simulated ratio of the circulating loop power and input power against proximity to critical coupling ΔK , for different losses α . (b) The corresponding maximum enhancement value against ΔK . Loop parameters are the same as in Fig. 1.

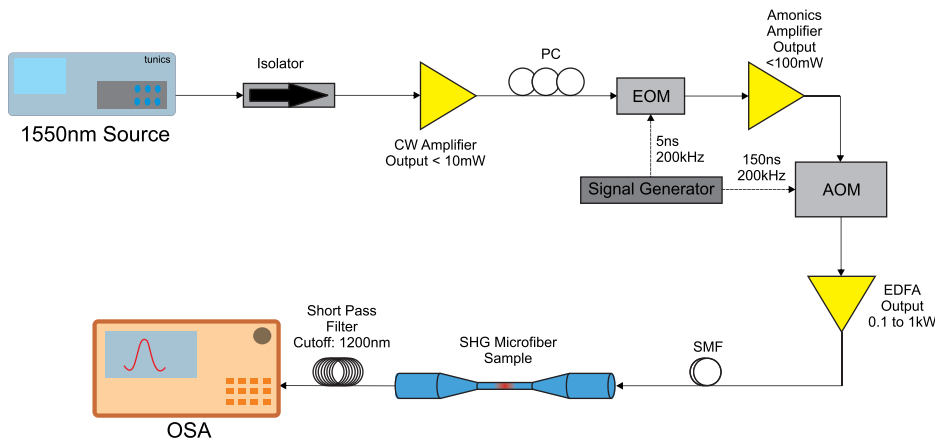


FIG. 3. Diagram of the source used during all study. The TLS could be detuned near the pump wavelength. Both EOM and AOM are synchronized and controlled by a signal generator. This source is connected to the sample, a straight MNF or a loop MNF resonator, with single mode fiber.

connected to a short pass filter (cut-off at $1.2\ \mu\text{m}$) with the output monitored on an optical spectrum analyzer (OSA). Tapering was then stopped when the SH signal was observed. The diameter of the uniform region of the produced MNF was measured to be $\sim 700\ \text{nm}$ as expected from simulations and the length of the taper was $20\ \text{mm}$, although the length L_{SH} over which the diameter was close to phase matching value ($\pm 1\ \text{nm}$) was approximately $200\ \mu\text{m}$ as measured by scanning electron microscopy.

At a peak-power of $P_0 = 90\ \text{W}$, the generated SH has an efficiency of $\eta = 2.5 \times 10^{-9}$, but the SH power would be expected to exhibit a quadratic dependency on the pump power.¹¹ This was indeed observed experimentally as shown in Fig. 4(b), where the pump power was varied while the SH was recorded. For example, when P_0 is increased by roughly 1.7 times to $150\ \text{W}$, the harmonic power is tripled to $P_{\text{SHG}} = 0.76\ \mu\text{W}$. However, since the efficiency only grows linearly with P_0 , the pump power must be significantly increased to achieve any noticeable gain, which may introduce issues with competing nonlinear effects such as unwanted spectral broadening in the preceding fiber.

On the other hand, it is possible to enhance the efficiency by increasing the length of the phase-matching region, i.e., either by producing a tapered fiber with a longer waist zone with the exact $780\ \text{nm}$ diameter or by producing

longer tapered fibers with a diameter smaller than the phase-matching diameter condition and generating SH on the taper transitions regions instead. Although it is possible theoretically, there are several limitations to manufacture such MNFs using the method described above. The final MNF length depends on the maximum travel limit of the linear stage as well as the heat profile of the heat source. For sources with a heat distribution along the fiber axis, a deviation of the diameter needs to be considered, changing the waist zone, final diameter and, accordingly, the taper profile.⁹ Moreover, small diameter fluctuations along the tapered fiber are expected by the heating method used to obtain the samples.^{12,13} Therefore, although longer tapered fiber could generate SH with better efficiency, it needs very precise fabrication, in order to minimize any of the possible issues listed above.

Alternatively, the efficiency could also be enhanced in short MNF while maintaining the low power pump input by introducing a loop resonator which incorporates the phase matched region of the MNF to locally increase the electric field near the phase-matching region and consequently improves the SHG signal by pump recirculation near resonance.

To demonstrate this, a $10\ \text{mm}$ long MNF sample was fabricated using the same method described earlier and used for SHG. When the sample was obtained, a loop was made

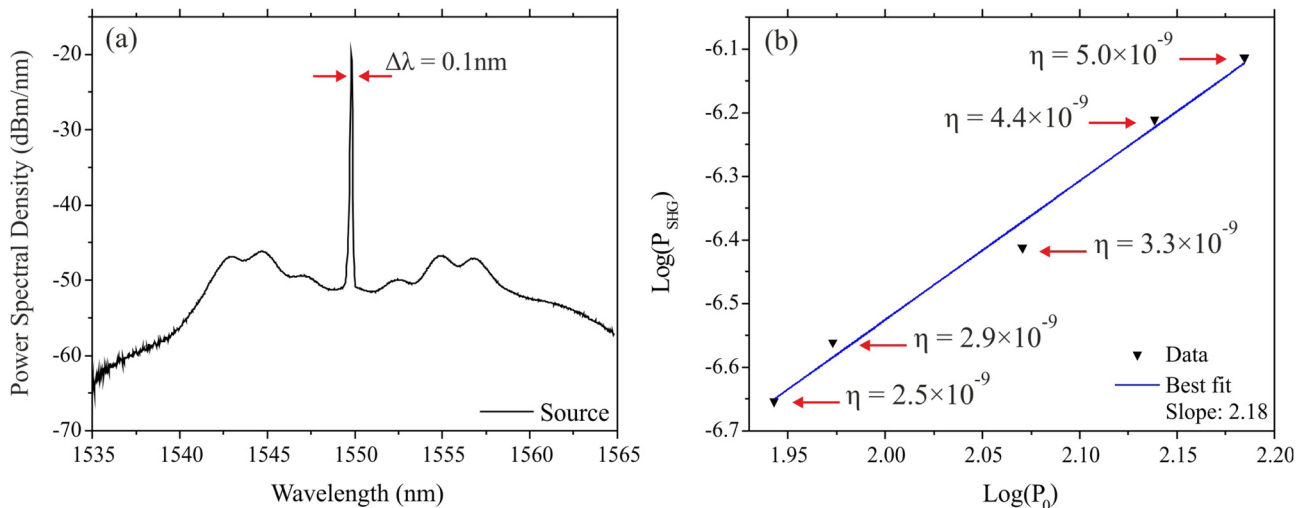


FIG. 4. (a) Spectrum of the $1.55\ \mu\text{m}$ laser source showing the $-3\ \text{dB}$ linewidth, characterized through a $-20\ \text{dB}$ coupler. (b) Investigation of the dependency between the generated second harmonic power P_{SHG} on the pump power P_0 . The linear fit slope shows the quadratic dependency between both signals' power.

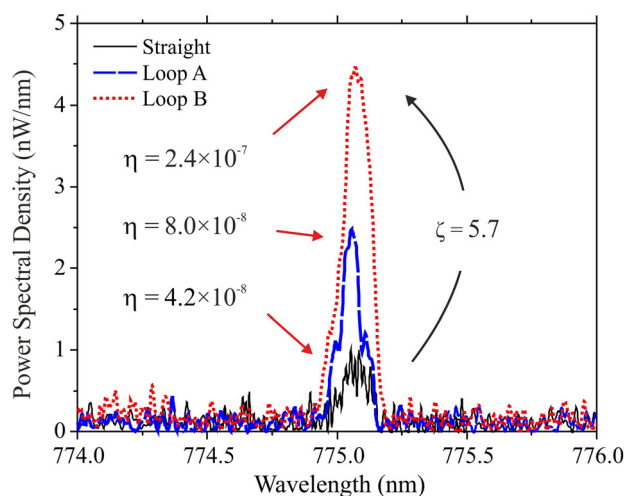


FIG. 5. SHG signal from the nonlinear loop resonator. The spectra show three signals from a same sample, the straight fiber SHG and other two just changing the loop diameter. Loop B shows an enhancement of 5.7 in comparison with the straight fiber.

by pushing and pulling both stages; the loop size and the coupling region could be changed by pulling the stages. For smaller loops, the coupling region is placed nearer to the thinner waist region with a stronger evanescent field, benefiting the coupling and resulting in an increased resonant electric field. If the pump is then tuned onto resonance, the circulating pump power and, consequently, the sample efficiency will be enhanced.

Spectra in Fig. 5 show the spectral density for three cases: for a MNF before making the loop and for two loops sizes A and B, with diameters of 4 and 1 mm, respectively. At a pump power of 90 W, an efficiency of 4.2×10^{-8} was calculated for the straight fiber and an efficiency of 2.4×10^{-7} for loop B, representing an enhancement of $\zeta = 5.7$ in comparison with the straight fiber case. The enhancement is lower than the aforementioned theoretical value, possibly due to a larger ΔK , or nonlinear pump broadening, which shifts some pump frequency components off resonance.

The enhancement from these preliminary results can be improved in future work by tuning the position of the nonlinear resonance to ensure it is closer to the pump wavelength. In addition, the enhancement depends on the coupling strength as shown in Fig. 2, and hence we can expect a higher efficiency using a longer coupling region to give an improved Q factor. Experimentally, loaded Q factors up to 1.2×10^5 have

been reported in Refs. 13 and 14, which would correspond to an enhancement of ~ 30 , assuming a loss of $\alpha = 10 \text{ m}^{-1}$. Yet higher Q factors are theoretically possible, and by using existing manufacturing technology it is reasonable to expect values approaching $Q \sim 10^6$, which would lead to an enhancement of roughly 2 orders of magnitude.

In conclusion, this study has shown SHG using microfibers and efficient enhancement using loop resonators. The nonlinear loop resonator theory for SHG has been demonstrated. Experimental results have evaluated the nearly linear dependency of the efficiency on the input pump power, which can be exploited to enhance SHG by just increasing the pump power. Based on this, the loop resonator has been shown as a device to increase locally the pump power at the SH phase-matching region and, therefore, increase the generated SH signal.

It is envisaged that in the future a greater SHG efficiency in such devices could be achieved by producing higher quality microfibers with a lower diameter deviation at the waist region, or by adding highly polarizable surface coatings to increase the surface nonlinearity.

G. Brambilla gratefully acknowledges the Royal Society (London, U.K.) for his University Research Fellowship. M. Gouveia gratefully acknowledges the Brazilian programme “Science without borders/CNPq,” provided by INCT-Fotonicom, for his scholarship.

¹Y. X. Fan, R. C. Eckardt, R. L. Byer, C. Chen, and A. D. Jiang, *IEEE J. Quantum Electron.* **25**, 1196–1199 (1989).

²U. Österberg and W. Margulis, *Opt. Lett.* **11**, 516–518 (1986).

³J. M. Dudley, G. Genty, and S. Coen, *Rev. Mod. Phys.* **78**, 1135–1184 (2006).

⁴T. A. Birks and Y. W. Li, *J. Lightwave Technol.* **10**, 432–438 (1992).

⁵T. Lee, Y. Jung, C. A. Codemard, M. Ding, N. G. R. Broderick, and G. Brambilla, *Opt. Express* **20**, 8503–8511 (2012).

⁶J. Lægsgaard, *J. Opt. Soc. Am. B* **27**, 1317–1324 (2010).

⁷S. Richard, *J. Opt. Soc. Am. B* **27**, 1504–1512 (2010).

⁸R. Ismael, T. Lee, M. Ding, N. G. R. Broderick, and G. Brambilla, *Opt. Lett.* **37**, 5121–5123 (2012).

⁹S. Pricking and H. Giessen, *Opt. Express* **18**, 3426–3437 (2010).

¹⁰V. Grubsky and A. Savchenko, *Opt. Express* **13**, 6798–6806 (2005).

¹¹C. Caspar and E. J. Bachus, *Electron. Lett.* **25**, 1506–1508 (1989).

¹²G. Agrawal, *Nonlinear Fiber Optics*, 4th ed. (Academic, San Diego, 2007), p. 499.

¹³C. Rodenburg, X. Liu, M. Jepson, S. Boden, and G. Brambilla, *J. Non-Cryst. Solids* **357**, 3042–3045 (2011).

¹⁴M. Sumetsky, Y. Dulashko, J. Fini, A. Hale, and D. DiGiovanni, *J. Lightwave Technol.* **24**, 242–250 (2006).